A. FATIGUE FAILURE IN ANNEALED Ti-6Al-4V MICROSTRUCTURES. B. FATIGUE LIFE IN ANNEALED AND MARTENSITIC Ti-6Al-4V

Charles M. Gilmore, et al

George Washington University

Prepared for:

Naval Air Systems Command

August 1975

THE
GEORGE
WASHINGTON
UNIVERSITY

STUDENTS FACULTY STUDY R
ESEARCH DEVELOPMENT FUT
URE CAREER CREATIVITY CC
MMUNITY LEADERSHIP TECH
NOLOGY FRONTIE ESIGN
ENGINEERING APP ENC
GEORGE WASHIN NIV

SCHOOL OF ENGINEERING
AND APPLIED SCIENCE

Security Classification

DOCUMENT CONTROL DATA - R & D

(Security classification of title, body of abstract and indexing annotation must be entered when the overall report is classified)

1. ORIGINATING ACTIVITY (Corporate author)	2a. REPORT SECURITY CLASSIFICATION
Institute for Fatigue, Fracture and Structural Reliability, The George Washington University	Unclassified
	2b. GROUP

3. REPORT TITLE

a. Fatigue Failure in Annealed Ti-6Al-4V Microstructures

b. Fatigue Life in Annealed and Martensitic Ti-6Al-4V

4. DESCRIPTIVE NOTES (Type of report and inclusive dates)

Technical Report

5. AUTHOR(S) (First name, middle initial, last name)

a. Charles M. Gilmore and M. Ashraf Imam

b. M. Ashraf Imam and Charles M. Gilmore

6. REPORT DATE	7a. TOTAL NO. OF PAGES	7b. NO. OF REFS
August 1975	a. 24 b. 16	a. 10 b. 8

8a. CONTRACT OR GRANT NO.	9a. ORIGINATOR'S REPORT NUMBER(S)
N00019-75-C-0093	II
b. PROJECT NO.	
c.	9b. OTHER REPORT NO(S) (Any other numbers that may be assigned this report)
d.	

10. DISTRIBUTION STATEMENT

Distribution unlimited

11. SUPPLEMENTARY NOTES	12. SPONSORING MILITARY ACTIVITY
	Naval Air Systems Command

13. ABSTRACT

a. The Fatigue crack initiation lives are determined for three annealed microstructures of Ti-6Al-4V: α-β annealed, recrystallized anneal and β anneal. The tests were conducted using fully reversed cyclic torsional strain amplitudes of ±0.006 and ±0.012. At both strain amplitudes the α-β annealed alloy had the longest fatigue life and the β annealed alloy had the shortest fatigue life.

Microscopic study of failed specimens showed that the fatigue crack initiation damage was localized to the vicinity of the α-β boundary; although in the different microstructures the appearance of the damage varied. A model is proposed to explain the accumulation of fatigue crack initiation damage. Microscopic study of crack propagation showed that extensive plastic deformation occurred around the crack in the α-β and recrystallized anneal microstructures. However, in the β anneal microstructure a mode of crack propagation was observed that resulted in no observable cracking or plastic deformation along the crack.

b. The fatigue life of annealed and quenched microstructures of the alloy Ti-6Al-4V were determined using a fully reversed cyclic torsional strain of 0.02. The quenched microstructures all had a longer fatigue life than the annealed microstructures, but a solution treatment of 1650°F followed by a water quench resulted in an alloy with a fatigue life four (4) times longer than any of the other solution treatments and

abstract for b continued on reverse side

DD FORM 1 NOV 1473

Security Classification

14. KEY WORDS	LINK A		LINK B		LINK C	
	ROLE	WT	ROLE	WT	ROLE	WT
Fatigue life, Titanium alloys, Ti-6Al-4V, Titanium martensite						

b. Abstract (continued)

and about ten times longer than the annealed specimens. The alloy solution treated at 1650°F has a microstructure of a β matrix containing fine martensite laths and islands of primary α within the β grains. The improved fatigue life of the specimens given the 1650°F solution treatment appears to result from the homogeneous nature of the microstructure relative to the other treatments. Most importantly the grain boundary β phase is not present in the alloy solution treated at 1650°F; it is at the grain boundary β-α interface that fatigue damage is often observed.

INSTITUTE FOR THE STUDY OF FATIGUE, FRACTURE AND STRUCTURAL RELIABILITY

a. Fatigue Failure in Annealed Ti-6Al-4V Microstructures

by C. M. Gilmore and M. A. Imam

b. Fatigue Life in Annealed and Martensitic Ti-6Al-4V

by M. A. Imam and C. M. Gilmore

SPONSORED BY:

Naval Air Systems Command

CONTRACT NO:

N00019-75-C-0093

TECHNICAL REPORT NO.

II

August 1975

SCHOOL OF ENGINEERING AND APPLIED SCIENCE
The George Washington University
Washington, D. C. 20006

Fatigue Failure in Annealed Ti-6Aℓ-4V Microstructures

by C. M. Gilmore and M. A. Imam

ABSTRACT

The fatigue crack initiation lives are determined for three annealed microstructures of Ti-6Aℓ-4V: α-β annealed, recrystallized anneal and β anneal. The tests were conducted using fully reversed cyclic torsional strain amplitudes of ±0.006 and ±0.012. At both strain amplitudes the α-β annealed alloy had the longest fatigue life and the β annealed alloy had the shortest fatigue life.

Microscopic study of failed specimens showed that the fatigue crack initiation damage was localized to the vicinity of the α-β phase boundary; although, in the different microstructures the appearance of the damage varied. A model is proposed to explain the accumulation of fatigue crack initiation damage. Microscopic study of crack propagation showed that extensive plastic deformation occurred around the crack in the α-β and recrystallized anneal microstructures. However, in the β anneal microstructure a mode of crack propagation was observed that resulted in no observable cracking or plastic deformation along the crack.

ic

LIST OF FIGURES

LIST OF TABLES

id

I. Introduction

Recent experiments have shown that changes in microstructure result in considerable changes in mechanical properties for titanium alloys.[1-7] At present most titanium alloy applications call for an annealed microstructure. Some of the annealing procedures that are being considered are the mill anneal (MA), α-β annealing ($\alpha\beta$A), recrystallized anneal (RA), and β anneal (βA). Specific procedures to obtain these anneal conditions are presented in the experiment section. Annealing of titanium alloys of course lowers the strength of the alloy, but it can increase the fracture toughness; however, the relationship between heat-treatment and other mechanical properties such as fatigue life is not well defined.

A goal of this research is to study the treatment of Ti alloys to produce alloys of improved fatigue life. The various thermal treatments of titanium alloys produce significantly different microstructures. Some work has been done on evaluating the fracture toughness of various thermal treatments for Ti alloys, but a thorough study of the crack initiation behavior of the annealed microstructures has not been reported. The alloy Ti-6Al-4V was chosen for this study because of its widespread use and because of the body of literature that exists on this alloy. The study will include the microstructural aspects of the crack initiation and propagation as well as the study of the fatigue lives.

II. Experiments and Results

A. Crack Initiation Life of Annealed Microstructures

In the study of fatigue crack initiation life of the alloy Ti-6Aℓ-4V the microhardness and fatigue life of several annealed microstructures were determined. All of these tests were conducted on a Ti-6Aℓ-4V alloy tube of .25 O.D. and .212 I.D. The composition for this alloy is in weight% :

Aℓ	V	O	H	C	N	Fe
5.8	4.4	.113	69 ppm	.02	.010	.08

The alloy was received in the mill annealed (MA) condition which consists of a final cold reduction of 25 to 30% followed by a vacuum anneal at 1475°F for 2 hours. The tube was cut into specimen lengths and the following annealing schedules were utilized:

<u>α-β anneal (αβA)</u>

800°C (1472°F) for 3 hours, furnace cool (FC) to 600°C (1112°F), followed by air cool (AC) to room temperature.

<u>Recrystallization Anneal (RA)</u>

928°C (1702°F) for 4 hours, FC to 760°C (1400°F) at 180°C/hour, FC to 482°C (900°F) at 372°C (702°F)/hour, AC.

β Anneal (βA)

0.5 hour at 1037°C (1900°F), AC to room temperature, 732°C (1350°F) for 2 hours, AC to room temperature.

All annealing was done in a vacuum of 10^{-5} mm Hg or better. In the above procedures furnace cooling refers to decreasing the power to the furnace to achieve the desired cooling rate; air cooling means that the heater is pulled away from the furnace and the furnace tube with specimens inside is air cooled. The specimens were metallurgically polished to a .1 microinch surface.

The microstructures resulting from the above annealing treatments are shown in Figures 1, 2 and 3. The treatments all result in a mixture of primary alpha and beta; however, the microstructure varies considerably. The microstructure of the αβA material has a matrix of primary alpha with particles of beta. The RA material has a matrix of recrystallized alpha with grain boundary β particles; however, the α and β grains are considerably larger than in the αβA material. Figure 3 shows the microstructure of the β anneal material. The alpha in the β annealed material is acicular, and the β phase forms in the acicular grain boundaries.

Microhardness measurements were made on each specimen with a Wilson Tukon Microhardness Tester using a Knoop Indenter with a load of 100 gm. The results shown in Table 1 are the average of 8 measurements except for the β annealed alloy which was tested 16 times because so much scatter was observed in the β annealed data. The standard deviation is noted in Table 1 so that the scatter in the β annealed data is evident. The reason

for the scatter in the annealed hardness data is not certain. The possibility of surface contamination was checked by grinding from the surface a few thousandths of an inch, but the same results were obtained. An important observation is the high average hardness of the α β annealed material relative to all of the other heat treatments.

The fatigue tests were conducted on machines developed by W.A. Wood. A cyclic torsional strain is applied to one end of the specimen through a lever system and the other end of the specimen is fixed with respect to twisting; however, the end of the specimen is free to elongate axially. In addition, it is possible to apply an axial stress to the specimen. In these tests an axial stress of 30,785 psi was applied because we were also investigating the interaction of fatigue and creep. The work on the fatigue creep interaction is reported elsewhere.[8] Measurement of the axial elongation provides a method for determining when a crack begins to propagate in the plane that is perpendicular to the axial load, for at that time the specimen begins to elongate. Thus in this study fatigue life is taken as the cycles to initition of a circumferential crack as indicated by an increased axial elongation of the specimen. The details of this measurement will be presented in another publication.[9]

In this study two cyclic strain amplitudes were used: ± 0.006 to produce high cycle fatigue lives on the order of 10^5 cycles, and ± 0.012 to produce low cycle fatigue lives on the order of 10^3 cycles. The results of the high cycle fatigue tests are presented in Table 2. The α-β anneal has the largest

average initiation life and the largest of the minimum lives to initiation (N_{Min}). The RA alloy is in the middle and the β anneal material has the shortest fatigue life. In these tests the fatigue life is the number of cycles to initiation of a circumferential crack. The results of the fatigue tests at a torsional strain of ±0.012 in Table 3 show that a similar ranking of life occurs at high strain amplitudes.

Crack Initiation and Microstructure

The crack initiation phase in all of the annealed alloys had common characteristics. In all cases the fatigue deformation was localized; and it was associated with phase or grain boundaries. The fatigue damage in the α-β annealed specimen cycled at ±0.012 shown in figure 4 is particularly informative. The fatigue damage has been revealed by etching with Kroll's reagent after cycling. The fatigue damage localizes in a narrow band that forms a crack into the specimen. But there is no apparent fatigue damage outside of this crack. This localized damage is entirely different than the highly dispersed fatigue damage that occurs in a plastic metal such as copper. In figure 4 the fractured β phase can be seen in the center of the microcrack. It appears from this photo that the presence of the β phase was an integral factor in the initiation of the microcrack.

In the recrystallized anneal alloy cycled at both ±0.006 and 0.012 shear strain amplitude the deformation was localized in the grain boundary β phase as is shown in figure 5. A transmission electron micrograph of the recyrstallized anneal alloy

in figure 6 shows that the recrystallized α phase is nearly dislocation free but the β phase has numerous defects. These defects are apparently the site of fatigue damage during the cyclic straining.

In the β annealed alloy the fatigue damage is also associated with the phase boundary as is shown in figure 7 for the specimen cycled at ±0.012 shear strain amplitude. The only difference observed between the specimens cycled at ±0.006 and ±0.012 is that the frequency of occurence of crack initiation sites is much larger in the specimen cycled at ±0.012; this was true for all alloy heat treatments.

Crack Propagation

In this study we were not able to determine the crack propagation rates, but we were able to make some microstructural observations on the specimens that should be of assistance in understanding the mechanism of crack propagation in titanium alloys.

The appearance of the damage associated with propagation of the crack was similar in the recrystallized and α-β annealed specimens; in the vicinity of the crack tip extensive plastic deformation and microcracking occurred. All along the crack extensive fatigue damage was present as is shown in figure 8 ; indicating a large amount of energy was dissipated during crack propagation. The only difference observed in the specimens cycled at ±0.006 and 0.012 shear strain was that the crack tip damage was more extensive at the higher strain amplitude.

The appearance of the fatigue cracks in the β annealed

material was significantly different than those in the RA and α-β annealed alloys. Figure 9 shows a photomontage of a microcrack in the β annealed alloy. The striking observation is that there is no significant deformation or cracking associated with propagation of the crack, the material adjacent to the crack is essentially unaltered by the passage of the crack tip. It does appear that the crack has been arrested by branching of the crack tip.

Study of the fatigue fracture surfaces also demonstrated that the recrystallized and α-β annealed alloys had similar crack propagation characteristics, the ductile fatigue striations shown in figure 10 are of the type observed on both the RA and αβA fatigue fracture surfaces. However, the β annealed specimen had areas of structure related crack propagation shown in figure 11, this type of fatigue fracture was not observed in either the recrystallized or α-β annealed specimens.

III Discussion

By studying several heat treatments of the alloy Ti-6Aℓ-4V we have been able to observe some common characteristics in the fatigue failure of these annealed α + β alloys. The fatigue crack initiation damage was localized to the grain or phase boundaries. The crack initiation damage in the recrystallized anneal alloy provided an extreme case because in this alloy the grain boundary β phase is quite large, measuring about 2μ across. The extensive deformation observed in the grain boundary β phase is indicative of the high stresses existing at the grain

boundaries of the anisotropic hexagonal α phase. Deformation was not observed in the β phase of the α-β and β annealed alloys because the β phase is quite small and highly constrained. Transmission electron microscopy may, however, be able to reveal the deformation if it does exist.

The longer fatigue life demonstrated by the α-β anneal alloy apparently results from its lack of extremes. In the recrystallized anneal alloy the β phase is large and fatigue damage localizes in the β phase. In the β annealed alloy the acicular microstructure is complex with many grains intersecting in complex ways. The stress at these complex intersections certainly must be high and these are then the potential sites for crack initiation. The α-β annealed alloy has neither of these characteristics, the β grains are small and the α grains are approximately equiaxed.

Observations of the microstructural characteristics of the fatigue damage, and some related observations on cyclic creep[8] have suggested the following mechanism for the initiation of fatigue cracking in this alloy. As a result of straining in one direction, dislocations move on some of the highly strained slip planes. During the motion through the crystal the dislocation encounters minor obstacles such as other dislocations that produce jogs. The jogged dislocations produce trails of vacancies as the dislocations move. Some dislocations are then stopped at an impenetrable obstacle, such as a grain or phase boundry. When the strain is reversed, the dislocations move in the opposite direction, away from the phase boundry, but obstacles well soon be encountered to stop the dislocation.

The strain in cyclic loading is again reversed to force the dislocations towards the phase and grain boundaries. As the jogged dislocations move to and from the phase boundary new sheets of vacancies are created. The vacancy sheet can be thought of as a long thin microcrack, and if many sheets of the vacancies are created by reversed motion of the dislocations in the vicinity of the phase or grain boundary then these can coalesce to form an even larger crack which would then be propagated by the cyclic strain. It would follow that if the phase boundary is the strongest barrier in the alloy, then many of the dislocations should eventually migrate to this barrier as they progressively overcome weaker barriers during the cyclic straining. The microcracks created by the coalescence of vacancies would etch up severely as shown in figures 4, 5 and 7. This could explain how the fatigue damage comes to be concentrated at the strong phase boundary during cyclic straining.

The crack propagation mode in the recrystallized and α-β annealed alloy exhibited extensive plastic deformation and microcracking in advance of the crack tip. However, in the β annealed alloy a mode of crack propagation was observed that had no apparent plastic deformation or microcracking along the crack path. This mode of propagation should be a low energy mode, it is similar in appearance to the "slipless" cracking observed in commercially pure titanium by Wood.[10] It is difficult to rationalize the observation of this apparent low energy mode of crack propagation with experimental data[1] that indicates the β annealed alloys have relatively slow crack propagation rates.

The explanation may lie in the number of microcracks. In the β annealed material many cracks and crack initiation sites are observed as in figure 12; however, in the recrystallized and α-β annealed alloys only one microcrack is usually observed, and this one grows to final failure. Thus in the β annealed alloy the energy of propagation must be spread over the many crack initiation and propagation sites. An individual crack may have a particularly low energy for propagation, but the strain energy is partitioned over many sites so that none of them grow at a particularly rapid rate. If this argument is a valid explanation of the relatively slow crack propagation rates in annealed titanium alloys; the desirability of this mechanism for producing a slow propagation rate must be given careful consideration. In comparison to an α-β annealed structure, the β annealed structure could be assumed to have many more crack initiation sites and microcracks as is demonstrated in figure 12. A crack in a structure that had been exposed to considerable service would have a difficult time competing with the myriad of microcracks and crack initiation sites already in the structure, and a slow fatigue crack propagation rate might be expected. However, it may not be necessary for the macrocrack to compete with the myriad of microcracks. If the macrocrack can grow by linking with the numerous microcracks, it is no longer necessary for the macrocrack to pass across the specimen, rather each existing microcrack only need grow a small distance to link up with its neighboring microcrack and the entire structure could be fractured by cracks that are individually

smaller than the minimum detectible crack size. This argument is of course hypothetical, but not unrealistic when applied to a material that is used because of its propensity to initiate cracks.

IV Summary

1. The α-β annealed alloy had the longest fatigue life followed by the recrystallized and beta annealed. The β annealed alloy relative to other treatments had a particularly short life at the shear strain of ±0.012.

2. The fatigue damage was localized to the boundaries in the α-β and β annealed alloys; the fatigue damage in the recrystallized anneal alloy occurred within the grain boundary β phase.

3. A model is proposed to explain the accumulation of fatigue damage at the grain and phase boundaries.

4. Crack propagation in the α-β and recrystallized anneal alloys occurred by extensive plastic deformation and microcracking at a single crack tip. In the β annealed alloy many microcracks were observed, and a low energy mode of crack propagation was observed with no apparent plastic deformation and microcracking along the crack path.

TABLE I
MICROHARDNESS OF ANNEALED SPECIMENS

ALLOY TREATMENT	KNOOP HARDNESS*	STANDARD DEVIATION
MILL ANNEAL	342.3	5.8
α-β ANNEAL	435.5	2.2
RECRYSTALLIZE ANNEAL	318.1	1.2
β ANNEAL	356.4	67.6

*BASED UPON 8 MEASUREMENTS EXCEPT FOR 16 MEASUREMENTS FOR THE β ANNEAL.

TABLE II
CYCLES TO CRACK INITIATION FOR A TORSIONAL STRAIN OF ±0.006

HEAT TREATMENT	MEAN	MINIMUM	STANDARD DEVIATION
α-β ANNEAL	84,370	73,690	9875
RECRYSTALLIZE ANNEAL	52,840	40,920	10,637
β ANNEAL	42,720	35,240	5684

BASED UPON FOUR SPECIMENS FOR EACH TREATMENT

TABLE III

CYCLES TO CRACK INITIATION FOR A
TORSIONAL STRAIN OF ±0.012

HEAT TREATMENT	MEAN	MINIMUM	STANDARD DEVIATION
α-β ANNEAL	9697	9110	386
RECRYSTALLIZE ANNEAL	6232	4560	1025
β ANNEAL	963	705	184

BASED UPON FOUR SPECIMENS FOR EACH TREATMENT

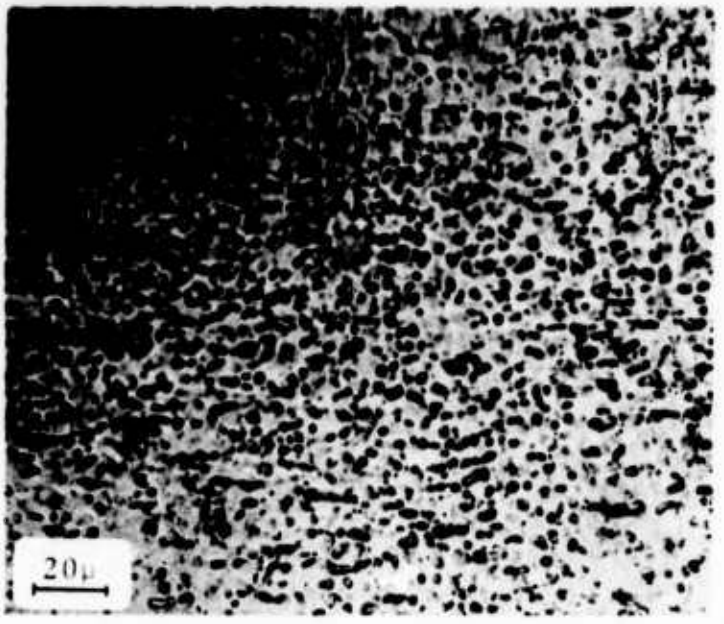

Figure 1. α-β annealed microstructure; light matrix is α, dark particles are β.

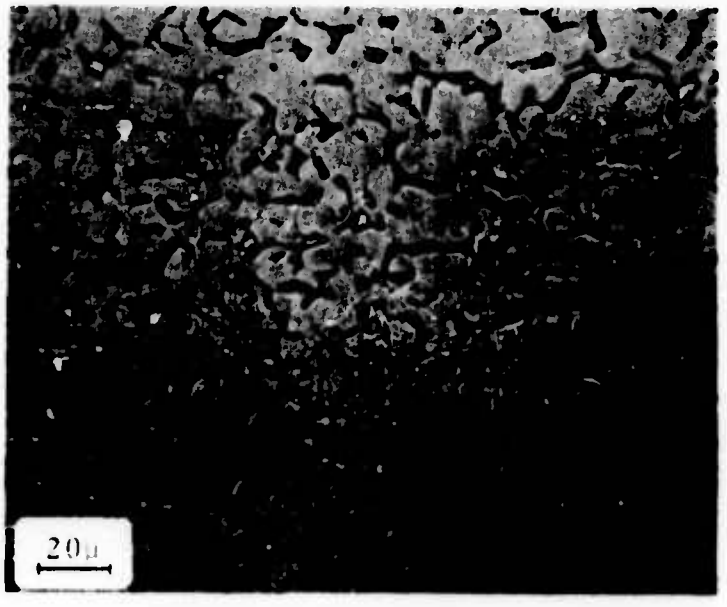

Figure 2. Recrystallized anneal microstructure, light equiaxed α grains, and dark grain boundary β.

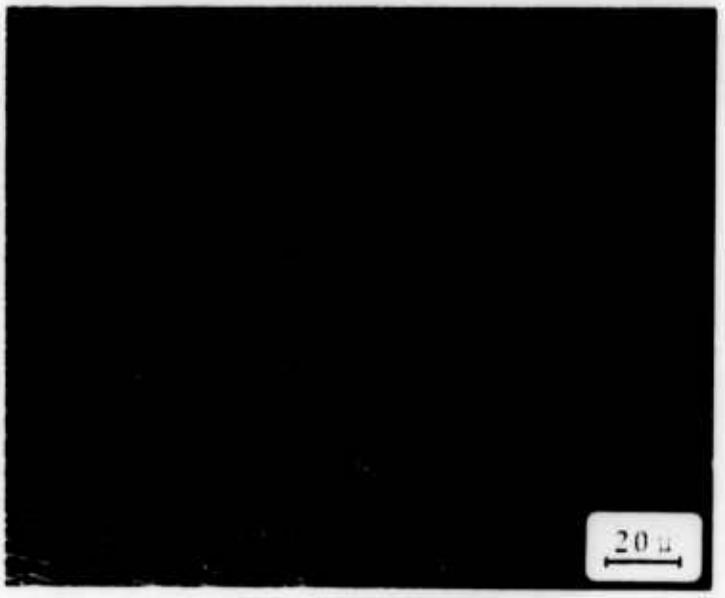

Figure 3. β annealed microstructure, acicular α with grain boundary β.

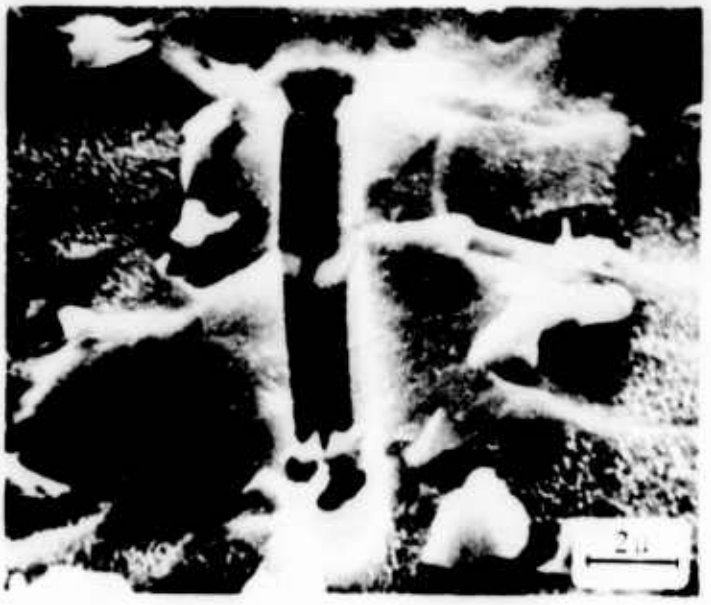

Figure 4. Fatigue damage in an α-β annealed specimen cycled at ±0.012 shear strain. Etched in Kroll's reagent.

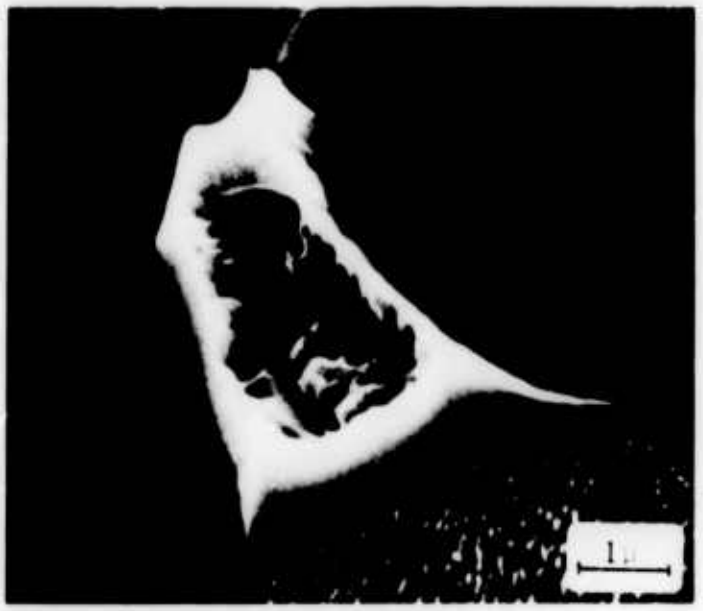

Figure 5. Fatigue damage in a recrystallize anneal specimen after cycling at ±0.012 shear strain. The fatigue damage is occurring in the β phase.

Figure 6. Transmission electron micrograph of the recrystallize anneal alloy. Primary α is nearly defect free, the β phase has numerous defects.

Figure 7. Fatigue damage in the β annealed specimen after fatigue at a shear strain of ±0.012.

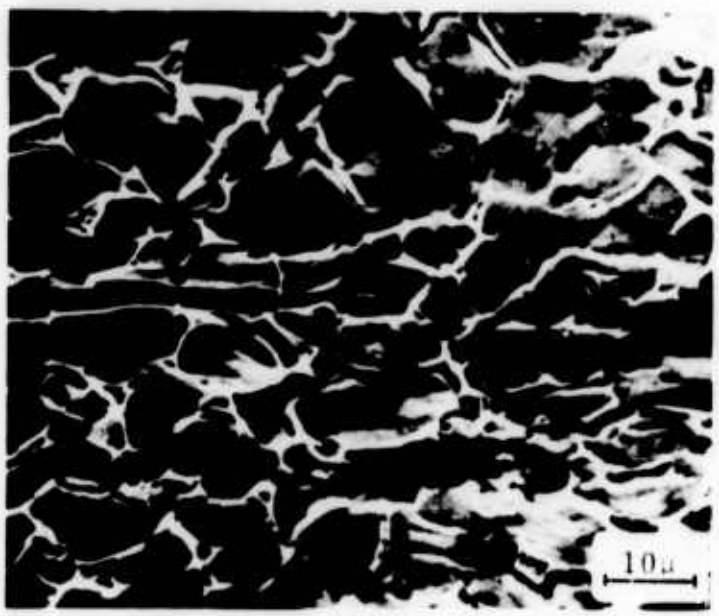

Figure 8. Deformation and microcracking in advance of the crack tip in the recrystallize anneal alloy cycled at a shear strain of ±0.012.

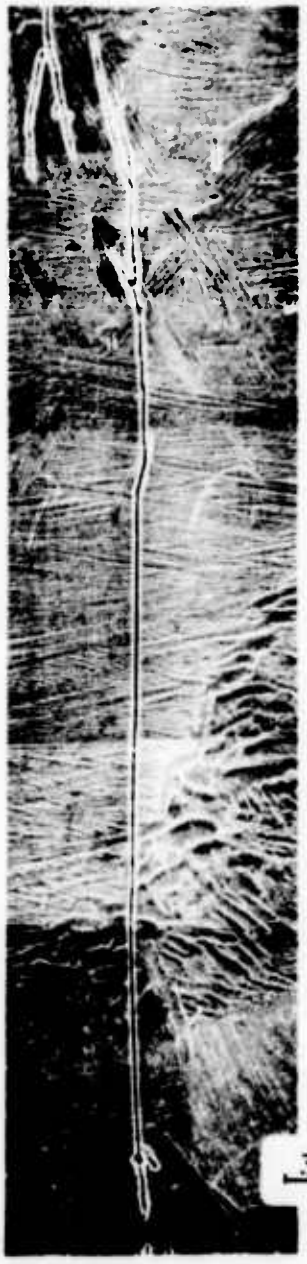

Figure 9. A fatigue crack in the β annealed alloy cycled to failure at a strain amplitude of ±0.012.

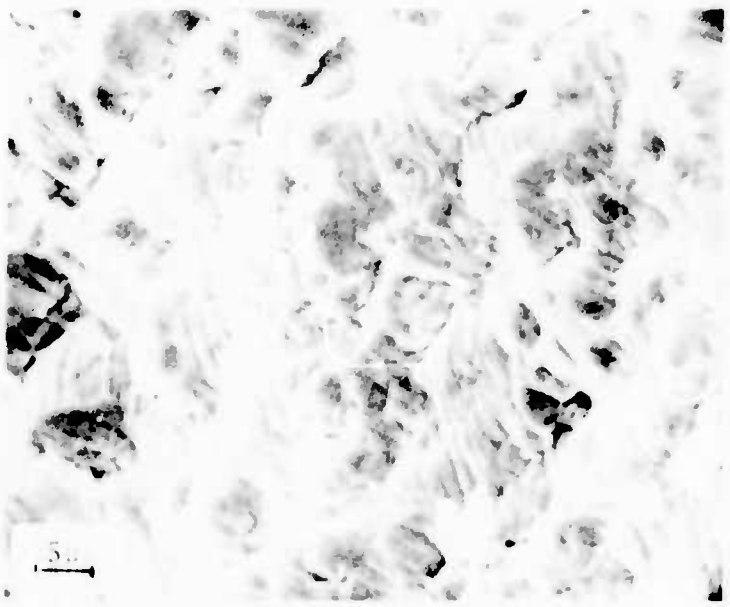

Figure 10. Well defined ductile fatigue striations on a RA stage II fracture surface after failure at a shear strain amplitude of ±0.006

Figure 11. Structure related fatigue fracture in β annealed material after failure at a shear strain of ±0.006.

Figure 12. Extensive microcracking in the β annealed alloy fatigued to failure at a shear strain of ±0.012.

LIST OF REFERENCES

1. M. J. Harrigan, M. P. Kaplan, and A. W. Sommer, 1972, Effects of Chemistry and Heat Treatment on the Fracture Mechanics Properties of Ti-6Aℓ-4V Alloy, Report NA-72-235.

2. M. F. Amateau, W. D. Hanna, and E. G. Kendall, 1971, The Effect of Microstructure on Fatigue Crack Propagation in Ti-6Aℓ-4V-2Sr Alloy, Materials Science Lab., Aerospace Corp., El Segundo, CA.

3. C. A. Stubbington and A. W. Bowen, 1974, Improvements in the Fatigue Strength of Ti-6Aℓ-4V through Microstructure Control, Journal of Materials Science, 9, 941-947.

4. P. E. Irving and C. J. Beevers, 1974, Microstructural Influences on Fatigue Crack Growth in Ti-6Aℓ-4V, Materials Science and Engineering, 14, 229.

5. J. M. VanOrden and L. L. Soffa, 1968, Effect of β Working on 6Aℓ-4V Titanium Alloy, A.S.M. T.R. No. D8-24.3.

6. M. A. Greenfield and H. Margolin, 1971, The Interrelationship of Fracture Toughness and Microstructure in a Ti-5.25ℓ-5.V-0.9 Fe-0.5Cu Alloy, Met. Trans., 2, 841.

7. F. A. Crossely and R. E. Lewis, 1973, Correlation of Microstructure with Fracture Toughness Properties in Metals, Report LMSC-D356114.

8. C. M. Gilmore and M. A. Imam, "Static and Cyclic Creep Properties of Ti-6Aℓ-4V for Several Heat Treatments," Institute for the Study of Fatigue, Fracture and Structural Reliability, The George Washington University, Report No. 21, 1975.

9. A. M. Freudenthal, C. M. Gilmore and M. A. Imam, in preparation.

10. W. A. Wood, 1974, Treatise on Materials Science and Technology, 5, 129.

Fatigue Life in Annealed and Martensitic Ti-6Aℓ-4V

by M. A. Imam and C. M. Gilmore

Abstract

The fatigue life of annealed and quenched microstructures of the alloy Ti-6Aℓ-4V were determined using a fully reversed cyclic torsional strain of 0.02. The quenched microstructures all had a larger fatigue life than the annealed microstructures, but a solution treatment of 1650°F followed by a water quench resulted in an alloy with a fatigue life four (4) times longer than any of the other solution treatments and about ten times longer than the annealed specimens. The alloy solution treated at 1650°F has a microstructure of a β matrix containing fine martensite laths and islands of primary α within the β grains. The improved fatigue life of the specimens given the 1650°F solution treatment appears to result from the homogeneous nature of the microstructure relative to the other treatments. Most importantly the grain boundary β phase is not present in the alloy solution treated at 1650°F; it is at the grain boundary β-α interface that fatigue damage is often observed.

LIST OF FIGURES

LIST OF TABLES

Introduction

Titanium alloys are known to have very good fatigue strength properties relative to other high strength metals such as aluminum and steel. Yet, in titanium there is still considerable potential for improving mechanical properties such as fatigue strength because of the multitide of possible microstructures that can result from varicus thermomechanical treatments of titanium. Most thermomechanical treatments of titanium alloys start with a solution treatment followed by a quench. In titanium alloys the high temperature β phase transforms upon rapid cooling into a martensitic structure. The martensite structure and the overall microstructure of the alloy are dependent upon the solution temperature and the cooling rate. The titanium microstructures will be discussed in more detail in the Alloy Characterization and Heat Treatment section. In thermomechanical treatments the quench is often followed by additional working or thermal treatment. However, in this work we are only going to study the effect of the solution temperature upon the resulting fatigue properties. There are several reasons for studying only this one variable. First if we are to understand the effect of microstructures upon titanium's mechanical properties we should study the variables one at a time. Secondly there have been some indications from previous work that martensitic microstructures in the as quenched condition may have some desirable mechanical properties. Quenched titanium is not brittle as is the martensite of iron and carbon. Fopiano et. al.[1] observed that in the alloy Ti-6Aℓ-4V martensite formation resulted in an increased strength without loss of ductility.

Crossley[2] has also observed that martensitic titanium alloys have a greater resistance to fatigue crack propagation than annealed microstructures, and they have good fracture toughness. No work to date, however, has been reported on the resistance of quenched martensitic microstructures to fatigue crack initiation. For small section use of titanium alloys the resistance to the initiation of microcracks can be more important than the crack propagation rate or the fracture toughness. Thus in this work we will study the life to failure of polished specimens of solution treated and quenched alloys, and we will compare the quenched alloys to annealed alloys. The titanium alloy Ti-6Aℓ-4V was chosen for this work because considerable research has been done on this alloy so a wealth of information exists on it. Also Ti-6Aℓ-4V is readily available in many forms, and the results are directly applicable to a service alloy.

Alloy Characterization and Heat Treatment

The alloy used in these fatigue life determinations was purchased from Alloy Specialties Inc. (HT No 600234-5357) as mill annealed solid 1/4 inch diameter rod with a composition in weight percent:

Aℓ	V	O	H	C	N	Fe
6.4	4.0	.141	55ppm	.01	.014	.18

The β transus of this alloy is 1805°F ±50°F. Specimens were water quenched after 10 minutes at solution temperatures of 1550°F, 1650°F, 1750°F and 1950°F. The solution treatment

was performed in a vertical air furnace; the suspended specimens were droped directly from the furnace into the water quench. After quenching an oxide affected surface layer of 0.020 inches was removed from the specimen radius. The specimens were metallurgically polished to produce a 0.1 microinch surface. Optical micrographs of quenched specimens etched in Kroll's reagent are shown in figures 1 to 4. Fatigue life specimens are not etched before testing, but after testing they are etched to reveal fatigue damage.

The fatigue life and microstructure of the quenched alloy is compared with the life and microstructure of an α-β annealed specimen. The α-β anneal was chosen because it has demonstrated greater fatigue lives than several other annealing treatments[3]. The α-β anneal is: 800°C(1472°F) for 3 hours, furnace cool to 600°C (1112°F), followed by air cool to room temperature. The optical microstructure resulting from the α-β anneal is shown in figure 5. Transmission electron microscopy reveals the microstructure shown in figure 6. The large areas are the primary α phase and the grain boundary phase is β; this was confirmed by selected area electron diffraction. The β phase is quite complex with numerous defects.

Transmission electron micrographs of specimens solution treated at 1950°F, 1650°F, and 1550°F are shown in figures 7, 8 and 9. According to other authors[5,6] Ti-6Aℓ-4V water quenched from a solution temperature of 1950°F transforms to the hexagonal α' martensite. The terminology suggested by Bagariatskii et. al.[4] is used in this paper. Selected area diffraction of the alloy

solution treated at 1950°F confirms that this is hexagonal martensite. Note the complex nature of the intersections of the martensite colonies shown in figure 7.

The specimen solution treated at 1650°F is shown in figure 8. The islands of dislocation free area index to be hexagonal primary α. Apparently this is primary α that was in equilibrium with β at the solution temperature. The matrix which is highly dislocated indexes to be β phase, but martensite reflections are present, and the dark field image in figure 10 shows the microstructure of the martensite. Unfortunately for Ti-6Al-4V it is not possible to differentiate between α' and α" from electron diffraction data, but according to the work of Williams et. al.[5,6] the martensite resulting from a quench at 1650°F solution temperatures should be α" possibly mixed with some α'. The α' and α" are structurally quite similar[7]. Thus the matrix of the alloy solution treated at 1650°F and quenched is composed of untransformed β mixed with fine martensite that transformed during the quench.

The alloy solution treated at the 1550°F temperature shown in figure 9 is a mixture of primary α that is relatively dislocation free and grain boundary β which is highly dislocated. No martensite reflections have been observed; they may be so weak that we have not been able to observe them. Thus the 1550°F solution treatment followed by a quench results in a mixture of primary α and grain boundary β which may have fine martensite that we have not been able to observe.

Experimental Determination of Fatigue Lives

The fatigue tests were conducted on machines schematically shown in figure 11. A cyclic torsional strain is applied to one end of the specimen through a lever system; the other end of the specimen is fixed with respect to twisting; however the end of the specimen is free to elongate axially. A constant axial stress can be applied to the specimen through a weight and pulley system, and in these tests an axial stress of 3060 psi was applied. The axial stress is applied to determine fatigue-creep interactions; this work will be presented in another report.

The fatigue tests were conducted with a fully reversed cyclic twist strain of ±0.02 at a frequency of 0.2 Hz. The fatigue life to final fracture is shown in Table 2. The most striking observation in the table is that all of the quenched microstructures show a significant increase in fatigue life relative to the annealed alloy. The second observation is that at a solution temperature of 1650°F there is a significant increase in fatigue life relative to the other solution temperatures. The changes in fatigue life must be related to the changes in microstructure; therefore, the fatigue life will be discussed in terms of the observed microstructures.

Discussion

At this time we can only speculate on the reason for the improvement in fatigue life that results from a quench at solution temperatures of about 1650°F; further studies must

be made of fatigued specimens to compare the fatigue damaged microstructures with the undamaged microstructures reported here. The microstructures produced by the various heat treatments are significantly different; and based upon past experience with the relationship of fatigue properties to microstructure we can speculate on the reasons for the changes in fatigue life that are observed.

The most striking result of the fatigue tests was the overall increase in the fatigue life of the quenched specimens relative to the annealed specimen. In previous work[8] we have shown that inelastic deformation resulting from cyclic straining of Ti-6Aℓ-4V concentrates in the grain and phase boundries. The α-β phase boundary in particular has been shown to be a location where fatigue microcracking initiates, an example of the type of damage observed is shown in figure 12. In the annealed Ti-6Aℓ-4V alloy the β phase forms in the α grain boundaries. The α grain boundaries would be expected to be regions of high strain mismatch because the hexagonal α grains are anisotropic. The grain boundary β lies in the region of high strain mismatch and it would be expected that large inelastic strains would occur at the α-β boundary resulting in fatigue damage.

In the alloy quenched from 1650°F the β in α grain boundaries has been eliminated. Possibly it is the mere elimination of β in α grain boundaries that has resulted in the increased fatigue life of this quenched microstructure. The alloy quenched from a solution temperature of 1650°F

had an increase in fatigue life by more than an order of magnitude relative to the annealed microstructure. As shown in figure 8 the microstructure of this quenched alloy is a mixture of α and β , but there are significant differences from the annealed two phase α plus β alloy. In the 1650°F quenched alloy the matrix is β. The β matrix is heavily dislocated and martensite needles are present as is shown (figure 10) in the TEM dark field image from one of the martensite reflections. These defects should provide considerable dislocation barriers in the β phase. The α phase forms islands within the β grains, the α is not a grain boundary α. Thus the α phase is strained within a homogeneous matrix, if we can consider the mixture of β and α' shown in figure 10 homogeneous. The absence of a grain boundary phase in the alloy quenched from a solution temperature of 1650° may be an important factor in its improved fatigue life.

The alloy quenched from a solution temperature of 1950°F had a fatigue life that was longer than the annealed specimens, but the life was shorter by a factor of four than the specimens solution treated at 1650°F. The quench from a 1950°F solution temperature results in a structure of martensite (α'), no grain boundary phase is present; but the microstructure is quite complex with many martensite laths intersecting at many different angles as shown in figure 7. It is likely that with this complex microstructure some regions of strain incompatibility would be observed. The microstructure of the martensite in the

specimen solution treated at 1650°F (figure 10) is quite different from that solution treated at 1950°F (figure 7).

The alloy solution treated at 1550°F and quenched (figure 9) has a microstructure quite similar to the α-β annealed material. (figure 6). Both are a mixture grain boundary β and primary α. The alloy solution treated at 1550°F may have martensite within the β phase, but this has not been confirmed. The reason for the increase in fatigue life in the 1550°F solution treated and quenched specimen relative to the α-β annealed specimen is not yet clear.

Summary

1. Solution treated and quenched microstructures demonstrated longer fatigue lives than annealed microstructures.

2. A solution treatment of about 1650°F resulted in a fatigue life about four (4) times as long as other solution treatments and about ten (10) times as long as the annealed microstructure.

3. The alloy solution treated at 1650°F has a microstructure of a matrix of β containing fine martensite laths, and islands of primary α within the β grains.

4. The improved fatigue life of the specimens given the 1650°F solution treatment appears to result from the homogeneous nature of the microstructure relative to the other treatments. Most importantly the grain boundary β phase is not present in the alloy solution treated at 1650°F; it is at the grain boundary β-α interface that fatigue damage is often observed.

REFERENCES

1. P. J. Fopiano, M. B. Bever and B. L. Averbach, 1969, Phase Transformations and Strengthening Mechanisms in the Alloy Ti-6Aℓ-4V, Trans. ASM, 62, 325.

2. F. A. Crossley and R. E. Lewis, 1973, Correlation of Microstructure with Fracture Toughness Properties in Metals, Report LMSC-D356114.

3. C. M. Gilmore and M. A. Imam, Improvement of Fatigue Properties in Titanium Alloys, 1974, Report No. 1 to Naval Air Systems Contract No. N00019-74-C-0086.

4. I. A. Bagariatskii, G. I. Nosova, and T. V. Tagunova, 1959, Factors in the Formation of Metastable Phases in Titanium-Base Alloys, Sov. Phys. Doklady, 3, 1014.

5. J. C. Williams and M. J. Blackburn, 1967, A Comparison of Phase Transformations in Three Commercial Titanium Alloys, Trans. ASM., 60, 373.

6. R. A. Spurling, C. G. Rhodes, and J. C. Williams, 1974, The Microstructure of Ti Alloys as Influenced by Thin Foil Artifacts, Met. Trans., 5, 2597.

7. A. B. Kolachev and V. S. Liasotskaya, 1973, The Structure and Properties of Quenched Titanium Binary Alloys, Titanium Science and Technology, eds. R.I. Jaffee and H. M. Burte, 3. 1569.

8. C. M. Gilmore and M. A. Imam, 1975, Static and Cyclic Creep Properties of Ti-6Aℓ-4V for Several Heat Treatments. Institute for the Study of Fatigue, Fracture and Structural Reliability, Report No. 21, The George Washington University.

TABLE I

MICROHARDNESS OF Ti-6Al-4V HEAT TREATED ALLOYS

HEAT TREATMENT †	KNOOP HARDNESS*	STANDARD DEVIATION
1550°F ST + WQ†	380	4.3
1650°F ST + WQ	450	7.1
1750°F ST + WQ	500	5.3
1950°F ST + WQ	511	0.0
α-β ANNEALED	435	1.5

†SOLUTION TREATMENT (ST) + WATER QUENCH (WQ)

*BASED UPON 8 MEASUREMENTS

TABLE II

FATIGUE LIVES OF HEAT TREATED Ti-6Aℓ-4V
ALLOYS CYCLED AT A SHEAR STRAIN OF ±0.02

HEAT TREATMENT	MEAN	MINIMUM	STANDARD DEVIATION
α-β ANNEAL	944	429	443
QUENCHED FROM 1550°F	2497	1837	717
QUENCHED FROM 1650°F	9616	8917	758
QUENCHED FROM 1950°F	2396	1633	487

BASED UPON FOUR SPECIMENS FOR EACH TREATMENT

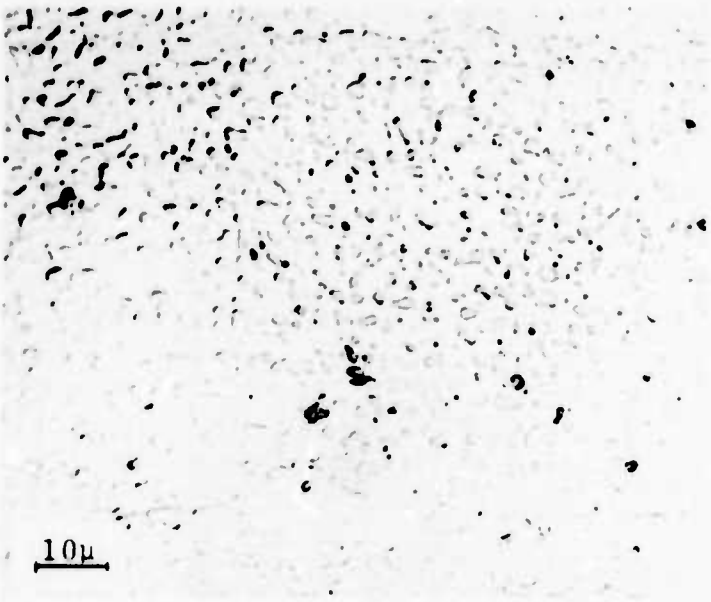

Figure 1. Optical Microstructure of a specimen water quenched from a solution temperature of 1550°F.

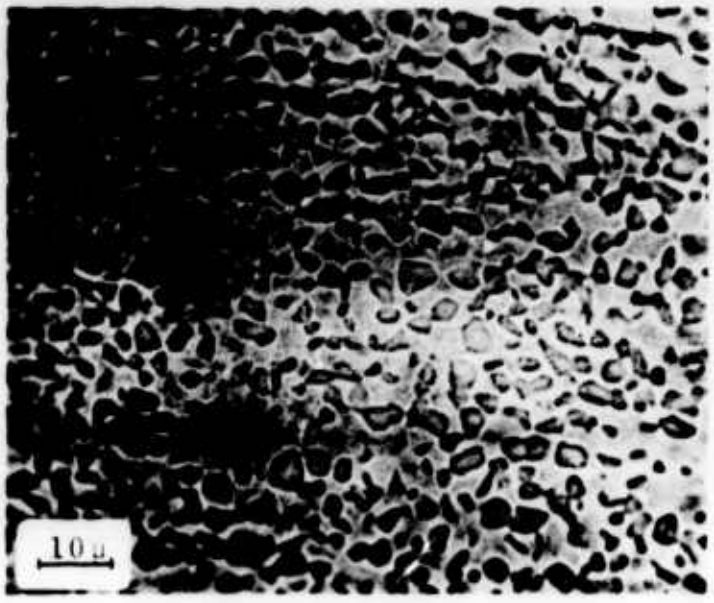

Figure 2. Optical Microstructure of a specimen water quenched from a solution temperature of 1650°F.

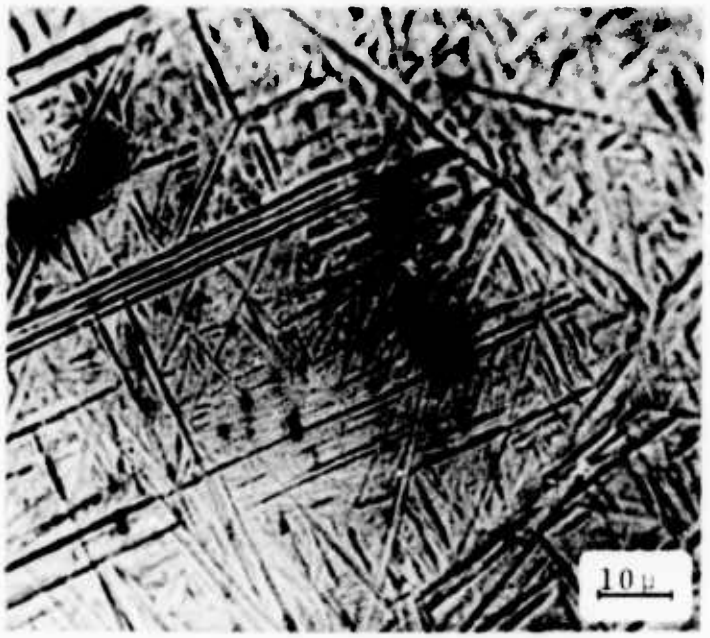

Figure 3. Optical Microstructure of a specimen water quenched from a solution temperature of 1750°F.

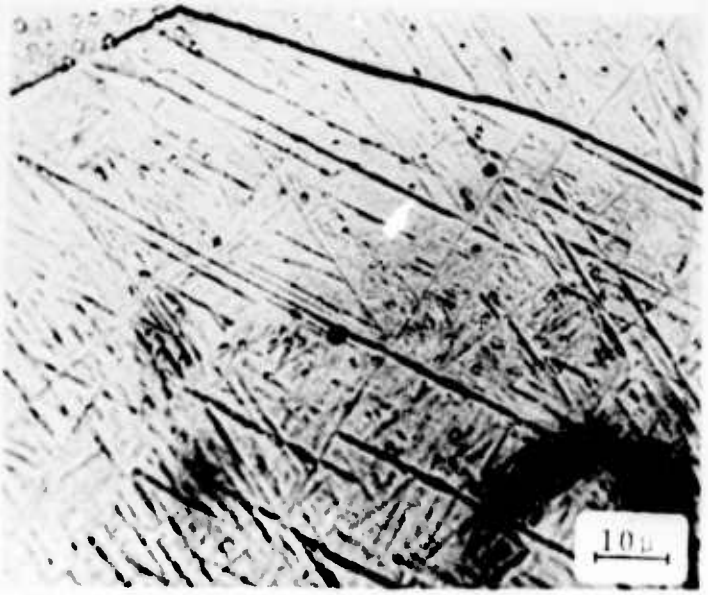

Figure 4. Optical Microstructure of a specimen water quenched from a solution temperature of 1950°F.

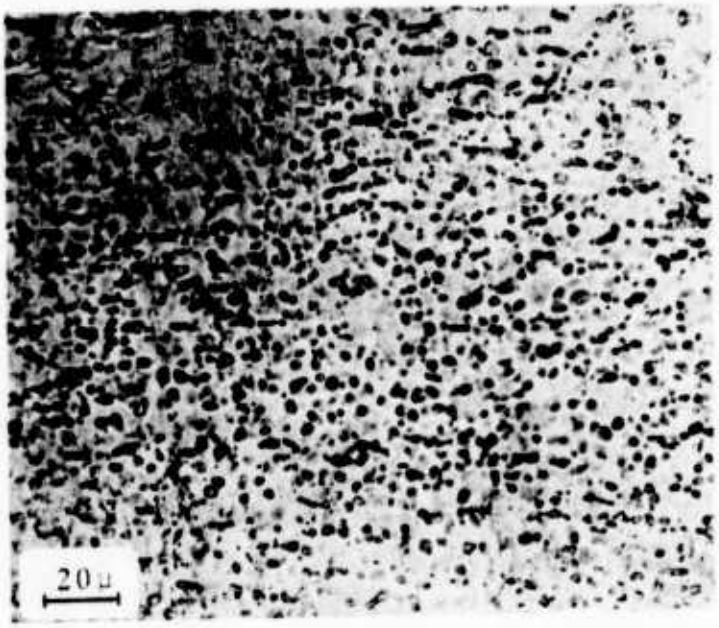

Figure 5. Optical Micrograph of a specimen α-β annealed.

Figure 6. Transmission electron micrograph of a specimen α-β annealed.

Figure 7. Transmission electron micrograph of the specimen quenched from 1950°F.

Figure 8. Transmission electron micrograph from the specimen quenched from 1650°F.

Figure 9. Transmission electron micrograph from the specimen quenched from 1550°F.

Figure 10. Dark field transmission electron micrograph of specimen quenched from 1650°F.

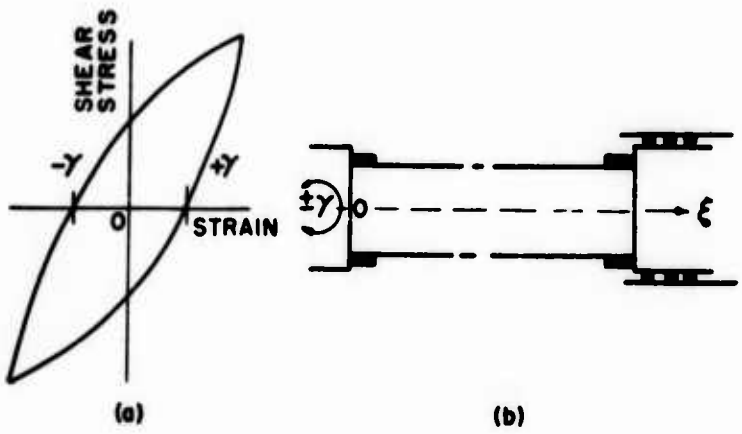

Figure 11. Schematic of the fatigue machine. A cyclic shear strain ±γ is applied to one end of the specimen. An axial load can be applied to the other end of the specimen and the end of the specimen is free to elongate.

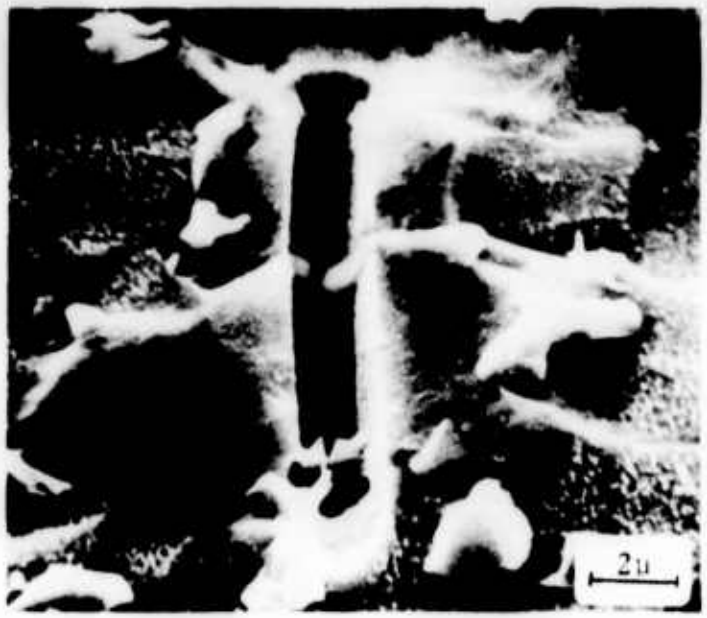

Figure 12. Fatigue microcracking associated with the interface in α β annealed Ti-6Al-4V after fatigue cycling at a shear strain of ±0.012.